Modeling the Sensitivity of Tropical Deep Convection to Changes in the Thermodynamic and Dynamic States

Zachary Eitzen[1,2] and Kuan-Man Xu[1]

1-NASA Langley Research Center; 2-Science Applications International Corporation

Introduction

For many years, clouds have been identified as one of the largest uncertainties in the simulation of climate change. In particular, there is still a large degree of uncertainty as to how cloud radiative forcing (CRF) and other cloud properties will change in a warmer climate.

Observations

- Cloud objects are diagnosed using edition 2B of the SSF product from the CERES instrument (Wielicki et al. 1996) on board the TRMM satellite.
- Deep convective (DC) cloud object selection criteria: cloud optical depth greater than 10, cloud height greater than 10 km, and 100% cloudy conditions within the footprint.
- This study is limited to the 68 large (effective diameter greater than 300 km) cloud objects observed over the tropical (25º S - 25º N) Pacific Ocean in March 1998.

Model

- The Advanced Regional Prediction System / Langley Research Center (ARPS/LaRC) model; based on ARPS (Xue et al. 2000).
- Includes Fu-Liou (1993) radiative transfer parameterization.
- Lin et al. (1983) microphysics scheme is used, modified following Krueger et al. (1995).
- Simulations performed in 2-D, run for 24 h, only last 12 h is analyzed.
- Periodic domain 512 km wide (Δx = 2 km) and 25 km high (stretched; average Δz = 500 m).
- Driven by advective cooling and moistening tendencies derived from ECMWF analyses.
- Five sets of 68 simulations performed: a control with observed SSTs and standard large-scale forcing, a set with the observed SSTs+2K, a set with the observed SSTs-2K, a set with the standard forcing+50%, and a set with the standard forcing-50%. This approach is similar to the "idealized sensitivity experiments" proposed in Bony et al. (2004).

Vertical profiles

Table 1: Pseudoadiabatic (PA) and reversible (R) CAPE

	Control	SST+2K	SST-2K	F+50%	F-50%
PA CAPE (12 hr)	981	1110	683	776	1342
PA CAPE (24 hr)	745	888	516	661	996
PA CAPE (12-24 hr avg)	827	962	579	686	1160
DC column weighted PA CAPE (12-24 hr avg)	733	874	512	605	1131
R CAPE (12 hr)	221	307	93	135	423
R CAPE (24 hr)	99	155	28	75	217
R CAPE (12-24 hr avg)	144	216	45	91	317
DC column weighted R CAPE (12-24 hr avg)	119	187	44	75	325

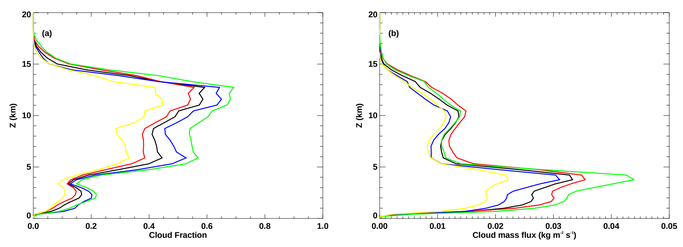

Fig. 1: Vertical profiles of (a) average cloud fraction and (b) cloud mass flux for the control simulations (black), SST+2K simulations (red), SST-2K simulations (blue), F+50% simulations (green), and F-50% simulations (yellow). Cloudy grid cells are defined where $\tau/\Delta z > 0.002$ m^{-1}.

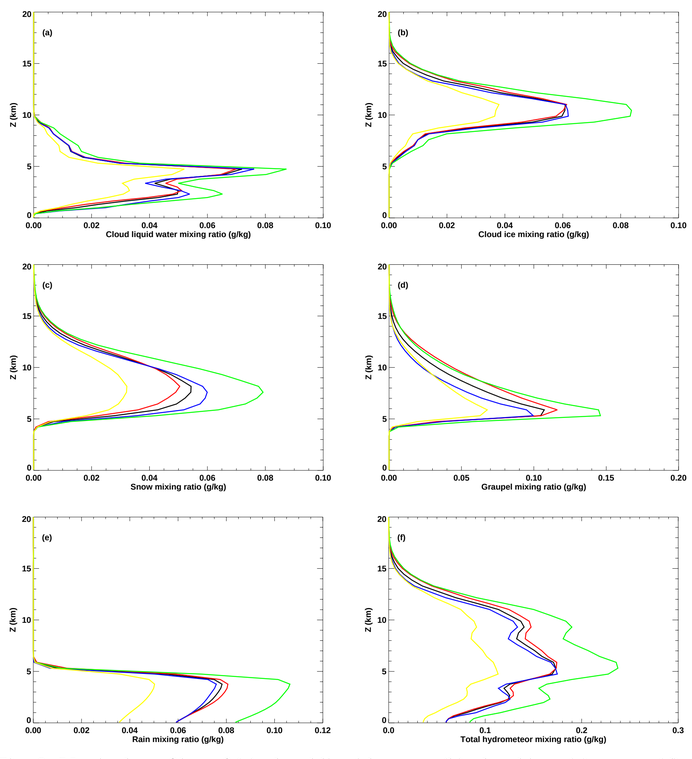

Fig. 2: Vertical profiles of (a) cloud liquid water; (b) cloud ice; (c) snow; (d) graupel; (e) rain; (f) the sum of (a)-(e) for the control (black), SST+2K (red), SST-2K (blue), F+50% (green), and F-50% (yellow) simulations.

Probability Density Functions of Cloud Properties

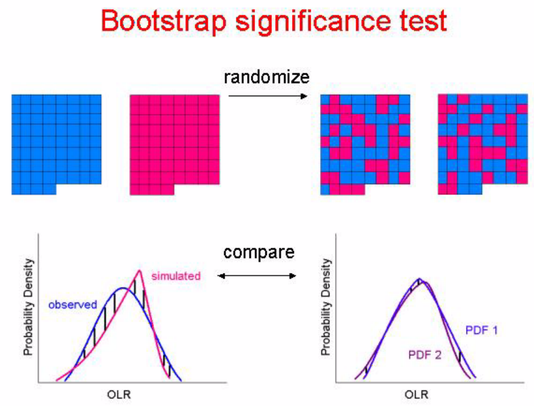

Fig. 3: Schematic diagram of the bootstrap approach. A measured L2 distance is calculated between PDFs comprised of data from two sets of 68 different cloud objects (left), and another L2 distance is calculated between two PDFs comprised of data from two sets of 68 cloud objects randomly chosen from the combined list of 136 (right).

Here, we are interested in the PDFs of columns that fulfill the selection criteria for deep convective clouds, as well as the PDFs for columns that have $\tau > 0.2$. The fractions of these two categories are shown in Table 2. Note that the fraction of deep convective columns relative to the fraction of other cloudy columns changes strongly with forcing, but changes only somewhat with SST The bootstrapping technique is applied to test for statistical differences between PDFs. See Fig. 3 for a schematic depiction of this process. The L2 (Euclidean) distance between two PDFs is measured and then compared to an 5000-member ensemble of L2 distances between pairs of PDFs constructed from random combinations of cloud objects from both of the original populations (Eitzen and Xu 2005). If less than 5% of the randomized L2 distances are larger than the measured L2 distance, then the PDFs are said to be different at the 5% level (indicated in red in Table 3).

Table 2: Deep convective and total cloud fraction

	Control	SST-2K	SST+2K	F-50%	F+50%
Total	0.894	0.934	0.868	0.800	0.946
Deep convective	0.227	0.252	0.205	0.129	0.344
Other	0.667	0.682	0.663	0.671	0.602

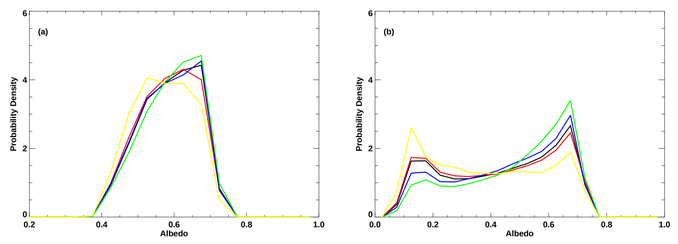

Fig. 4: Distributions of albedo for (a) deep convective columns; (b) cloudy columns produced by the control (black), SST+2K (red), SST-2K (blue), F+50% (green), and F-50% (yellow) simulations.

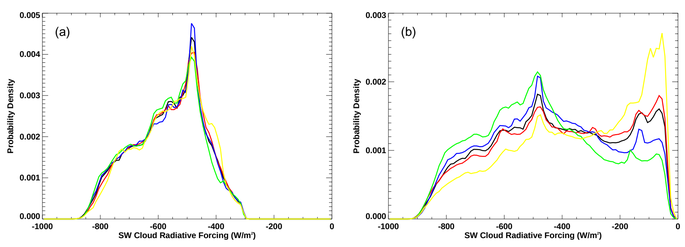

Fig. 5: Same as Fig. 4, except for shortwave CRF.

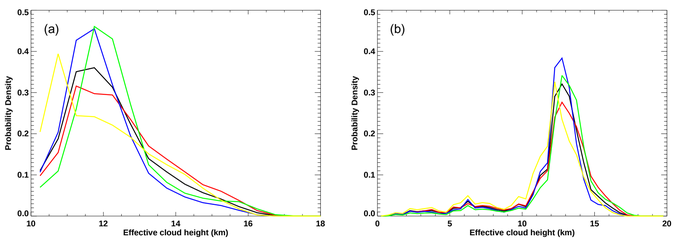

Fig. 6: Same as Fig. 4, except for cloud top height.

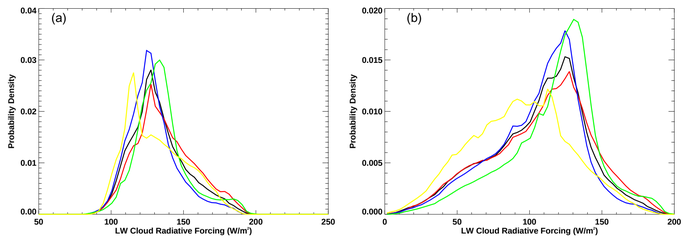

Fig. 7: Same as Fig. 4, except for longwave CRF.

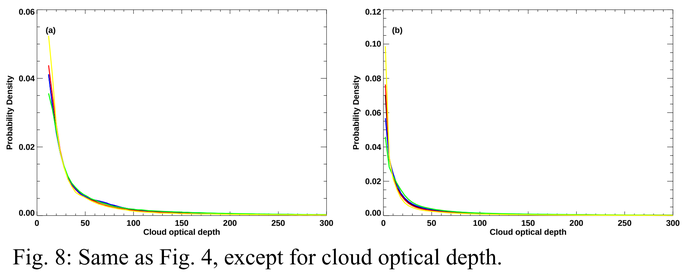

Fig. 8: Same as Fig. 4, except for cloud optical depth.

Table 3: Bootstrap probabilities

	Deep convective clouds		All clouds	
	SST-2K vs. SST+2K	F-50% vs. F+50%	SST-2K vs. SST+2K	F-50% vs. F+50%
albedo	0.7482	0.0230	0.0474	0.0000
cloud top temperature	0.1172	0.0000	0.0044	0.0004
cloud height	0.0336	0.0000	0.0008	0.0000
OLR	0.0950	0.0004	0.1000	0.0000
snow and ice path	0.0318	0.0608	0.4340	0.0000
optical depth	0.5438	0.0188	0.0044	0.0000
SW CRF	0.9936	0.8002	0.2036	0.0000
LW CRF	0.0232	0.0006	0.0364	0.0000
total CRF	0.9670	0.8524	0.0388	0.0000

Multilayer Clouds

Table 4: Percentages of multilayer clouds

	Control	SST-2K	SST+2K	F-50%	F+50%
clear	10.6	6.6	13.2	20.0	5.4
1 layer cld	50.5	46.7	52.3	50.2	50.0
2 layer cld	30.8	35.1	28.3	24.1	34.4
3 layer cld	7.2	10.2	5.7	5.1	9.1
4+ layer cld	0.8	1.4	0.6	0.6	1.1

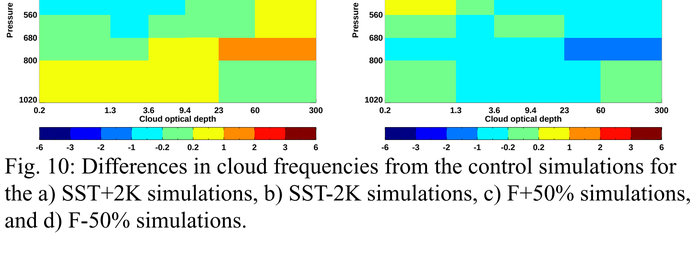

Fig. 9: (a) The simulated cloud frequencies for the control simulations, where the optical depth of each column is calculated by integrating from the top of the atmosphere to the surface. (b) Same as (a), except that optical depths are now calculated separately for each vertically contiguous cloudy region within the columns.

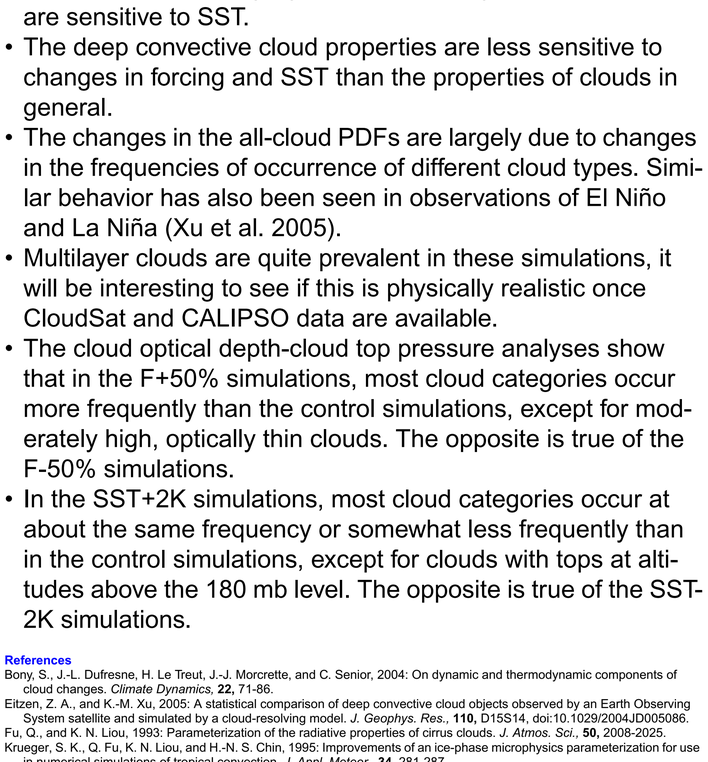

Fig. 10: Differences in cloud frequencies from the control simulations for the a) SST+2K simulations, b) SST-2K simulations, c) F+50% simulations, and d) F-50% simulations.

Conclusions

- The cloud properties produced by the F+50% and F-50% simulations are generally more different from control than those produced by the SST+2K and SST-2K simulations, although the OLR and related properties of the deep convective clouds are sensitive to SST.
- The deep convective cloud properties are less sensitive to changes in forcing and SST than the properties of clouds in general.
- The changes in the all-cloud PDFs are largely due to changes in the frequencies of occurrence of different cloud types. Similar behavior has also been seen in observations of El Niño and La Niña (Xu et al. 2005).
- Multilayer clouds are quite prevalent in these simulations, it will be interesting to see if this is physically realistic once CloudSat and CALIPSO data are available.
- The cloud optical depth-cloud top pressure analyses show that in the F+50% simulations, most cloud categories occur more frequently than the control simulations, except for moderately high, optically thin clouds. The opposite is true of the F-50% simulations.
- In the SST+2K simulations, most cloud categories occur at about the same frequency or somewhat less frequently than in the control simulations, except for clouds with tops at altitudes above the 180 mb level. The opposite is true of the SST-2K simulations.

References

Bony, S., J.-L. Dufresne, H. Le Treut, J.-J. Morcrette, and C. Senior, 2004: On dynamic and thermodynamic components of cloud changes. *Climate Dynamics,* **22,** 71-86.

Eitzen, Z. A., and K.-M. Xu, 2005: A statistical comparison of deep convective cloud objects observed by an Earth Observing System satellite and simulated by a cloud-resolving model. *J. Geophys. Res.*, **110,** D15S14, doi:10.1029/2004JD005086.

Fu, Q., and K. N. Liou, 1993: Parameterization of the radiative properties of cirrus clouds. *J. Atmos. Sci.*, **50,** 2008-2025.

Krueger, S. K., Q. Fu, K. N. Liou, and H.-N. S. Chin, 1995: Improvements of an ice-phase microphysics parameterization for use in numerical simulations of tropical convection. *J. Appl. Meteor.*, **34,** 281-287.

Lin, Y.-L., R. D. Farley, and H. D. Orville, 1983: Bulk parameterization of the snow field in a cloud model. *J. Climate Appl. Meteor.*, **22,** 1065-1092.

Wielicki, B. A., B. R. Barkstrom, E. F. Harrison, R. B. Lee III, G. L. Smith, and J. E. Cooper, 1996: Clouds and the Earth's Radiant Energy System (CERES): An Earth Observing System experiment. *Bull. Amer. Meteor. Soc.,* **77,** 853-868.

Xu, K.-M., T. Wong, B. A. Wielicki, L. Parker, and Z. A. Eitzen, 2005: Statistical analysis of satellite cloud object data from CERES. Part I: Methodology and preliminary results of the 1998 El Niño/2000 La Niña. *J. Climate*, in press.

Xue, M., K. K. Droegemeier, and V. Wong, 2000: The Advanced Regional Prediction System (ARPS) - A multiscale nonhydrostatic atmospheric simulation and prediction tool. Part I: Model dynamics and verification. *Meteor. Atmos. Physics.*, **75,** 161-193.